The human remains from Axlor (Dima, Biscay, Northern Iberian Peninsula)

Asier Gómez-Olivencia[a,b,c*]

Diego López-Onaindia[d]

Nohemi Sala[e,c]

Antoine Balzeau[f,g]

Ana Pantoja[c]

Ignacio Arganda-Carreras[h,b,i]

Mikel Arlegi[a,j]

Joseba Rios-Garaizar[e]

Aida Gómez-Robles[k,l,m]

[a]Dept. Estratigrafía y Paleontología, Facultad de Ciencia y Tecnología, Universidad del País Vasco-Euskal Herriko Unibertsitatea (UPV/EHU). Barrio Sarriena s/n, 48940 Bilbao, Spain.

[b]IKERBASQUE. Basque Foundation for Science.

[c]Centro UCM-ISCIII de Investigación sobre Evolución y Comportamiento Humanos, Avda. Monforte de Lemos 5 (Pabellón 14), 28029 Madrid, Spain.

[d]GREAB, Unitat d'Antropologia Biològica, Departament de Biologia Animal, Biologia Vegetal i Ecologia, Facutat de Biociències, Universitat Autònoma de Barcelona, 08193 Bellaterra, Spain.

[e]Centro Nacional de Investigación sobre la Evolución Humana (CENIEH), Paseo de la Sierra de Atapuerca 3, 09002 Burgos, Spain.

[f]Équipe de Paléontologie Humaine, UMR 7194, CNRS, Département Homme et Environnement, Muséum national d'Histoire naturelle. Musée de l'Homme, 17, Place du Trocadéro, 75016 Paris, France

[g]Department of African Zoology, Royal Museum for Central Africa, Tervuren, Belgium

[h]Dept. Ciencias de la Computacion e Inteligencia Artificial. Facultad de Informatica, Universidad del País Vasco-Euskal Herriko Unibertsitatea (UPV/EHU) Manuel Lardizabal Ibilbidea 1, 20018 Donostia, Gipuzkoa, Spain.

[i]Donostia International Physics Center (DIPC). Manuel Lardizabal Ibilbidea 4, 20018 Donostia, Gipuzkoa, Spain.

[j]Université de Bordeaux, PACEA UMR 5199, Bâtiment B8, Allée Geoffroy Saint-Hilaire, 33615 Pessac, France.

[k]Department of Anthropology, University College London, WC1E 0BW London, UK.

[l]Department of Genetics, Evolution and Environment, University College London, WC1E 6BT London, UK.

[m]Department of Life Sciences, Natural History Museum, SW7 5BD London, UK.

Correspondence

Asier Gómez-Olivencia, Dept. Estratigrafía y Paleontología, Facultad de Ciencia y Tecnología, Universidad del País Vasco-Euskal Herriko Unibertsitatea (UPV/EHU). Barrio Sarriena s/n, 48940 Bilbao, Spain.

Email: asier.gomezo@ehu.eus (A.G.-O.)

Abstract

Objectives: We provide the description and comparative analysis of all the human fossil remains found at Axlor during the excavations carried out by J.M. Barandiarán from 1967 to 1974: a cranial vault fragment and eight teeth, five of which likely belonged to the same individual, although two are currently lost. Our goal is to describe in detail all these human remains and discuss both their taxonomic attribution and their stratigraphic context.

Materials and methods: We describe external and internal anatomy, and use classic and geometric morphometrics. The teeth from Axlor are compared to Neandertals, Upper Paleolithic and recent modern humans.

Results: Three teeth (a left dm^2, a left di^1, and a right I_1) and the parietal fragment show morphological features consistent with a Neanderthal classification, and were found in an undisturbed Mousterian context. The remaining three teeth (plus the two lost ones), initially classified as Neandertals, show morphological features and a general size that are more compatible with their classification as modern humans.

Discussion: The combined anatomical and stratigraphic study suggest that the remains of two different adult Neandertals have been recovered during the old excavations performed by Barandiarán: a left parietal fragment (level VIII) and a right I_1 (level V). Additionally, two different Neandertal children lost deciduous teeth during the formations of levels V (left di^1) and IV (right dm^2). In addition, a modern human individual is represented by five remains (two currently lost) from a complex stratigraphic setting. Some of the morphological features of these remains suggest that they may represent one of the scarce examples of Upper Paleolithic modern human remains in the northern Iberian Peninsula, which should be confirmed by further testing.

KEYWORDS

Neandertal, anatomically modern humans, enamel-dentine junction, geometric morphometrics, Paleolithic

1-Introduction

The rock-shelter of Axlor is located in the mountainous region included in the national park of Urkiola (Biscay, Basque Country) and preserves one of the most important Middle Paleolithic sequences in the northern Iberian Peninsula (Figure 1). Axlor was discovered in 1932 by the Basque prehistorian J. M. Barandiarán. The first archaeological excavations took place in 1967, and encompassed a total of eight field seasons until 1974 (Barandiarán, 1980). These excavations revealed a sequence of nine layers (I-IX), in which Middle Paleolithic lithic assemblages were found in levels III to VIII. Recent excavations (2000-2008) directed by González-Urquijo, Ibáñez and Rios-Garaizar, provide a new stratigraphic sequence, roughly equivalent to the previous one, but with additional levels, not previously identified or excavated by Barandiarán. Some of these levels were deposited before level VIII, but their chronology remains uncertain (González-Urquijo, Ibañez, Lazuén & Mozota, 2014; Rios-Garaizar, 2017). Additionally, an early Upper Paleolithic occupation has been recognized (level A of the new excavations, equivalent to the base of Barandiarán's level II, previously considered sterile; González-Urquijo et al., 2014). Ultra-filtered dates obtained from red deer with anthropogenic marks from level IV have yielded results that go beyond the radiocarbon limit, correcting previous dating which situated this level at the very end of regional Middle Paleolithic (Marín-Arroyo et al., 2018). Across the sequence, there are clear differences in terms of the technological characteristics, percentage of ungulate taxa consumed, and type of occupation of the cave between the upper (III-VI) and lower levels (VII-VIII) of the Mousterian sequence, which has been confirmed during the recent excavations (Altuna, 1989; Castaños, 2005; González-Urquijo et al., 2014; Rios-Garaizar, 2017). Recent reassessment of the Barandiarán collection has identified the presence of bird and carnivore exploitation for the first time during the Middle Paleolithic of the Cantabrian region: at least a golden eagle and a lynx where exploited for dietary purposes (Gómez-Olivencia et al., 2018a).

[INSERT FIGURE 1 HERE]

The current human fossil record published for Axlor is limited to five upper left dental remains (C, P^4-M^3) with a maxilla fragment, likely belonging to the same individual (a young adult), which were found in 1967 from a level with Quina Mousterian lithics and faunal remains of red deer, reindeer, and steppe bison (Basabe, 1973; Figure 2). Basabe (1973) seems to be cautious in the taxonomic assessment of these remains. While he considers that the morphology of these dental remains is compatible with that found in similar (Mousterian) archaeological contexts, he nonetheless considers these remains as "evolved", with "intermediate" size and traits, including the "unclear" taurodontism in M1-M2 (Basabe, 1973). Currently, only three (P^4, M^1, M^3) of these remains are curated at the Arkeologi Museoa (Bilbao), whereas the location of the other teeth is unknown. A more recent reassessment of these teeth supported a Neandertal classification based on their size and the alleged presence of taurodontism in the molars (Rostro-Carmona, 2013). However, a visual inspection of the morphology of the M^1 shows that it does not present the typical Neandertal morphology for this tooth (e.g., Bailey, 2004; Gómez-Robles et al., 2007). Moreover, no study of the internal anatomy of the teeth based on virtual anthropology techniques has been performed, which could provide a more accurate taxonomic assessment. In 2005, the re-assessment of the whole Barandiarán collection (coordinated by J.E. González Urquijo) resulted in the recognition of three additional human remains: two teeth and a cranial fragment. More recently, the reassessment of the faunal collection from Barandiarán's excavation has resulted in the identification of an additional human remain among the faunal remains: an upper deciduous molar.

[INSERT FIGURE 2 HERE]

Here we provide a detailed description and comparative analysis of all the human fossil remains from Axlor found during J.M. Barandiarán's excavations, including a taphonomic analysis

of the cranial fragment. This study also reassess the taxonomic affinities of the remains published by Basabe (1973) and Rostro-Carmona (2013), and discusses the archaeological context of all the human remains from this collection. In fact, the revision of the archaeological context from the field-notes taken by J.M. de Barandiarán at the site casts doubts on the stratigraphic position of all the teeth studied by Basabe (1973) and Rostro-Carmona (2013), while in the rest of the cases the association of these human remains to Mousterian contexts seems secure (Supplementary Information Text S1).

2-Materials and Methods

2.1-Materials

The current collection of human remains from the Barandiarán excavations includes an upper fourth premolar, an upper first molar and an upper third molar from the same (young adult) individual (Basabe, 1973), a cranial fragment, a lower right central incisor, an upper left first deciduous incisor and a left upper deciduous second molar (Table 1). Their spatial location, according to the available information is shown in Figure 2. Access to these materials was granted by the Arkeologi Museoa (Bilbao). The CT scans of these fossils and the derived segmentation files and 3D volumes are accessible via XXX.

[Note to the Editor and the reviewers: All the original micro-CTs and the derived segmentation files and 3D volumes will be made accessible in a public repository (e.g., morphosource or figshare) and the corresponding DOIs will be included in the next version of this manuscript.]

[INSERT TABLE 1 HERE]

2.2-Micro-CT scanning

All the Axlor human remains were micro-CT scanned at the Spanish National Research Center for Human Evolution (CENIEH) using a Phoenix v/tome/x s (GE Measurement & Control). The resolution was maximized depending on the size of the different fossil remains (teeth: 18.99µm; cranial fragment: 33µm).

2.3-Anatomical descriptions

Standard methods were used to describe and analyze the external and internal anatomy of the cranial fragment. Previous knowledge of the anatomy and relative variation of exo and endocranial surfaces was used to identify the anatomical position and diagnostic features of the cranial fragment (e.g., Balzeau, 2013; Balzeau, Grimaud-Hervé & Gilissen, 2011; Balzeau et al., 2017). The teeth were described following the stablished anatomical dental terms (Carlsen, 1987). In addition, we scored several non-metric traits following both the Arizona State University Dental Anthropology System (ASUDAS) (Turner, Nichol & Scott, 1991) and some complementary traits described by Bailey (2002), which were compared to Neandertals, Upper Paleolithic modern humans (UPMH) and recent humans (Martinón-Torres, Bermúdez de Castro, Gómez-Robles, Prado-Simón, & Arsuaga, 2012). Some of these traits were also scored in the EDJ surface and completed by the traits described by Martin, Hublin, Gunz, & Skinner (2017) for the molars. The roots of the incisors were measured following the method described by Le Cabec, Gunz, Kupczik, Braga & Hublin (2013): Root Length (RL), Root Volume (RV), Root Pulp Volume (RPV), Crown Pulp Volume (CrPV) and different ratios between these measurements. Dental wear assessment was based on Molnar (1971).

2.4-Bone thickness mapping (cranial fragment) and volume segmentation (teeth)

The 3D variation of the total bone thickness of the cranial fragment was evaluated using the exo- and endocranial surfaces using the module Surface-Distance of Avizo 7. The results of this analysis were illustrated using a chromatic scale and compared to previous studies (Balzeau, 2013) in order to gain insights on the potential taxonomic significance of the thickness distribution pattern.

In the case of the teeth, before their segmentation, the CT image volumes were pre-processed using Fiji (Schindelin et al., 2012) by first converting them to 8-bit and then re-sampling them in the Z direction by a factor of 2 (final volume resolution: 0.019 x 0.019 x 0.038 microns per voxel). Next, the volumes were segmented using an interactive learning approach (Arganda-Carreras et al., 2017) that classified each voxel as belonging to one of the following classes: bone, dentine, enamel, or background. The pulp chamber was afterwards labeled by semi-automatic filling of the cavity inside the other teeth labels. The output label images were cleaned up by removing small artifacts and noise by means of morphological operations (Legland, Arganda-Carreras & Andrey, 2016). Finally, we performed manual correction of the segmented images using AvizoLite software due to the presence of cracks in some teeth, and lower density zones in the enamel some of the teeth.

2.5-Taphonomic analysis

The cranial bone was macroscopically and microscopically examined using a hand lens and a stereoscopic zoom microscope (Olympus SZX10) to examine surface modifications. For the analysis of striae regarding the differentiation between cut marks and trampling marks we have used the protocol proposed by Domínguez-Rodrigo, de Juana, Galán & Rodríguez (2009). The cranial breakage pattern was analyzed following the criteria developed by Sala, Pantoja-Pérez, Arsuaga, Pablos & Martínez (2016) to assess the presence/absence of perimortem (fresh bone) and postmortem (dry bone) fractures. Four parameters were recorded: fracture outline (linear, depressed,

stellate); fracture angle (right or oblique); fracture edge (smooth or jagged); presence/absence of cortical delamination.

2.6-Geometric morphometrics

Geometric morphometric analyses of the occlusal surface of the premolar and molar crowns were used to compare the Axlor posterior permanent teeth with the Neandertal and modern human samples used in Gomez-Robles et al. (2007), Gómez-Robles, Bermúdez de Castro, Martinón-Torres, Prado-Simón, & Arsuaga (2012), and Gómez-Robles, Martinón-Torres, Bermúdez de Castro, Prado-Simón, & Arsuaga (2011). Modern human samples included both fossil and recent modern humans. Occlusal photographs were used to place 2D configurations of landmarks and semilandmarks. For the M^1, analyses were repeated on the original photographs and on an occlusal projection of the occlusal surface obtained after virtually correcting enamel cracks. Because the Axlor M^1 is heavily worn, the location of anatomical landmarks on cusp apices cannot be unequivocally determined. Therefore, M^1 analyses were repeated twice, using the original configuration of landmarks and semilandmarks as described in Gómez-Robles et al. (2007) and only the configuration of outline semilandmarks (after removing the four anatomical landmarks). The second analysis, therefore, focuses on the ability of the M^1 occlusal outline to differentiate Neandertal from modern human molars. The Axlor P^4 and M^3 are substantially less worn than the M^1, so only the complete configuration of landmarks and semilandmarks was evaluated for them. For all the posterior teeth, geometric morphometric analyses were performed that included and excluded size variation (in form and shape space, respectively). A discriminant analysis based on the first ten principal components of shape variation was carried out to evaluate the species that Axlor teeth are assigned to.

3-Metric, morphological and taphonomic description

The cranial and the dental remains are described here. The comparison of the external crown metric data between Axlor teeth and different comparative samples are shown in Table 2. Only taxonomically useful metric traits are discussed below.

[INSERT TABLE 2 HERE]

3.1-Cranial remain

AX.11B.415.400 is a fragment (56 × 41 mm) of a left parietal bone, which preserves 54 mm of the sagittal suture (Figure 3). The suture is not fused, and this left fragment has been separated from the right parietal bone without any breakage of the indentations. Bone thickness for the analyzed area is only slightly smaller than in La Ferrassie 1 (Balzeau, 2013) and thus incompatible with a young immature status. Thus, the fragment is not from a child, but may belong to a young adult or adult. The antero-posterior curvature of this fragment is not very pronounced.

[INSERT FIGURE 3 HERE]

Bone thickness distribution was quantified on nearly the whole preserved area of this fragment. Thickness varies between 3.4 mm and 10.5 mm. Mean thickness of the fragment is 5.4 mm. Thickness is evenly distributed along the surface of the fragment, there is no clear increase or decrease related to bone thickness variation. The only exception concerns the blood vessels on the endocranial surface of the anterior border of the fragment, which are associated with a clear thinning of the bone (the area with white dots at the anterior border of the bone, noted V on Figure 3). Moreover, the infero-anterior corner of the fragment shows a slight increase in bone thickness (represented by the purple area, noted PC on Figure 3) which continues posteriorly and obliquely. It corresponds to the postcentral sulcus.

Some clear endocranial features are visible. Some branches of the meningeal system are noticeable. They probably all belong to the anterior ramus, one being the anterior branch (noted A on Figure 3), the second corresponding to the obelic branch (noted O on Fig. 3). The anterior branch splits in two simple veins that are quite large. The obelic branch splits into two smaller and long veins. Concerning the gyral pattern visible on this endocranial surface, two sulci are clear. The course of the postcentral sulcus (noted PC on Figure 3) goes from the antero-inferior corner of the fragment to the center of the medial border of the fragment. This sulcus is well printed and shows a clear course. Anteriorly, the central sulcus (noted C on Figure 3) seems to run along the course of the most anterior vein of the anterior ramus. Those two sulci have a parallel course, delimiting a post-central gyrus that has a regular width on its preserved extension.

Both bone thickness distribution pattern and endocranial anatomy provides information that helps to propose a taxonomic attribution for this fragment. Bone thickness shows little variation. In modern humans, there is a clear decrease in bone thickness in the area of the superior parietal gyrus. The pattern observed on this fragment resembles what has been described for Neandertals (Balzeau, 2013). The position and size of the anterior branch of the meningeal system on this fragment, as well as its subsequent bone thickness variation, fits with the anatomy observed in Neandertals. The meningeal system in this area has more anastomoses than in modern humans, and blood vessels are thinner and more numerous (Grimaud-Hervé, 1997). In summary the anatomical features preserved in this parietal fragment are consistent with a Neandertal classification.

The bone surface of the cranial remain is well preserved and does not show weathering (sensu Behrensmeyer, 1978). No direct carnivore activity (i.e., tooth marks) was documented, nor any sign of burning. Similarly, no other biological modifications, such as rodent activity or root etching, was observed. This cranial fragment shows several striations in the outer table in five

different areas (Figure 4). In some cases, the grooves are close "V" shaped, but microstriations were not evident. On the other hand, the trajectories of the grooves are usually sinuous and most of the bone surface is covered by very shallow striae. In some cases, the color of the striations is lighter compared with the bone surface suggesting that they have occurred after its deposition. These observations are compatible with trampling marks following the protocol described by Domínguez-Rodrigo et al. (2009). Regarding the fracture analysis, this remain displays three linear fractures, one of them parallel and two perpendicular to the cranial suture. The two fractures perpendicular to the suture have right angled edges, jagged surfaces and absence of cortical delamination. These characteristics are typical of fracturing in dry bone (Sala et al., 2016). However, the fracture that is parallel to the suture displays an oblique angle, smooth surface and presence of cortical delamination (0.75 cm) on the inner table. The combination of these fracture attributes is usually considered representative of perimortem fractures (Sala et al., 2016).

[INSERT FIGURE 4 HERE]

3.2-Upper left fourth premolar, maxillary fragment with upper first molar and upper third molar belonging to the same individual

Descriptions and analyses are provided for the three dental remains belonging to the same individual. These remains are shown in Figure 5 and are morphologically compared in Tables 3-5.

Ax.13F.265.1 (AX.13E/13F.265-270.1 according to the museum records) is a complete premolar, although its root is damaged and presents longitudinal cracks on both sides and some smaller transversal cracks. In addition, there is a small pitting on the vestibular side of the buccal cusp, and erosion on the tip of this cusp (Figure 5). Also, in the areas with the highest enamel thickness of the crown (the buccal and lingual sides) there is a part of the enamel that shows lower

density in the CT images (Supplementary information Figure S12). The similarity in height between the lingual and buccal cusps and the two long inter-proximal facets suggest it is a P^4. In addition, the distal interproximal wear facet matches well the mesial counterpart of the Axlor M^1 (Figure 5), further supporting that this is a P^4, and indicating that they both belonged to the same individual (see below).

[INSERT FIGURE 5 HERE]

The occlusal surface is moderately worn (stage 3; Molnar, 1971), and the dentine is exposed on the lingual cusp. Yet, the inter-proximal wear facets are visible to the naked eye, and the distal one is larger. This premolar shows a distal accessory marginal tubercle, a bifurcated buccal essential crest (grade 2 from Bailey, 2002) and a distal accessory ridge on the buccal cusp (Table 3).

[INSERT TABLE 3 HERE]

At the EDJ level, two major cusps are observed: buccal and lingual. The essential crest of both the lingual and buccal cusps are bifurcated (Grade 2; Table 3), which are features typically observed on Neandertals (92.3% and 61.5% respectively). On the mesial side it presents a continuous transverse crest that does not connect with the horn tip of the lingual cusp, also typical in Neandertals (69.2%). In addition, there is an intermediate accessory marginal tubercle distal to the buccal cusp. The coronal pulp cavity is conformed by the two horns corresponding to the main cusps, where the buccal horn is almost two times larger than the lingual one.

This premolar shows a single, mediolaterally flat root. This root runs wide and straight in the most cervical half, while the apical third is narrower. Both the mesial and distal sides present longitudinal grooves, of which the distal is more pronounced. The analysis of the root canal based

on the µCT images shows that this is a single canal (Type $1R_1$) which is only found in 12.5% of Neandertals (Pan & Zanolli, 2019; Table 3).

Geometric morphometric analyses show that Neandertals and recent modern humans are almost completely separated along the P^4 morphospace, with Neandertals showing a lingually expanded and asymmetric morphology and modern humans showing a symmetric and lingually reduced configuration, where the interfoveal distance is strongly reduced (Figure 6; Gómez-Robles et al., 2011). Interestingly, fossil modern humans completely overlap with Neandertals, showing a premolar configuration that is much more similar to that of Neandertals than to that of recent modern humans. The Axlor P^4 plots right on the imaginary line that separates the areas of distribution of Neandertals and recent modern humans, but outside the range of distribution of both groups. The Axlor P^4 plots on this intermediate position because it shares a generally asymmetric morphology with Neandertals, but a moderately reduced distal cusp and a shortened interfoveal distance with modern humans. Based on these traits, a discriminant analysis classifies the Axlor P^4 as a modern human, but with a low probability of only 56%. When adding size information, the Axlor P^4 plots again in an intermediate position between Neandertals and recent modern humans. Interestingly, it also plots on the lower extreme of the size variation found in fossil modern humans, indicating that the Axlor P^4 is larger than most recent modern humans, but smaller than most Neandertals and fossil modern humans.

[INSERT FIGURE 6 HERE]

Ax.13F.265.3 (AX.13E/13F.265-270.3 according to the museum records) represents a left maxilla fragment, preserving both the external surface (ca. 13.3 × 9.2 mm), and the internal surface (13.4 × 9.8 mm), with the left M^1 placed in its alveolus. This tooth is fragmented due to longitudinal

and transversal cracks that affect the crown and roots (Figure 5). Inter-proximal wear facets are clear in both sides and the mesial one shows clear grooves on it. This mesial facet shows two chippings in its occlusal border. Also, the occlusal surface of the tooth is heavily worn (stage 4-5; Molnar, 1971) and the dentine is exposed in all four main cusps, which interferes with the observation of several morphological traits.

The metacone and the hypocone of this molar are well developed (grade 4 ASUDAS), and there is no cusp 5 (Table 4). The hypocone is not distolingually projected, but it is aligned with the protocone on the lingual side and with the metacone on the distal side. Due to the heavy occlusal wear, it is not possible to score the presence of Carabelli's tubercle or the mesial marginal accessory tubercle. The EDJ reveals the presence of an intermediate post-paracone tubercle and no sign of fifth cusp (Table 4). Moreover, there is a type II *crista obliqua*, continuously connecting the metacone to the protocone, which is centrally positioned. The occlusal wear also affects the dentine to a large extent, which may influence trait assessments, but a Carabelli's tubercle does not seem to be present. The horn tip of the hypocone pulp cavity is small and not projected, in contrast with the typical Neandertal morphology (Supplementary Information Figure S14).

[INSERT TABLE 4 HERE]

The three roots are separated, all the radicular canals are divergent and the body is relatively short. The canal corresponding to the mesio-buccal root is the widest one, being mesiodistally flat. Moreover, the cervical third of this root canal is elongated, presenting a wide morphology, and the apical end is bifurcated. This root morphology contrasts with the typical Neandertal taurodont configuration.

Analyses of shape variation show a generally clear separation between Neandertals and modern humans, with Neandertals showing a skewed M^1 configuration and modern humans showing a squared configuration (Figure 6; Bailey, 2004; Gómez-Robles et al., 2007). Both groups show a minor overlapping area where many fossil modern humans, as well as the Axlor M^1, are found. Based on shape data, Axlor M^1 is classified as a modern human with a probability of 88.8% or 98.6% (before and after correcting the enamel cracks, respectively). Because of the small size of the Axlor M^1, adding size information to the PCA makes this specimen plot comfortably within the modern human range of distribution.

When assessing only the M^1 outline as defined by curve semilandmarks (Supplementary Information Figure S15), the differentiation between Neandertals and modern humans is less clear. There is still an area of the morphospace occupied only for Neandertals and another one occupied only by modern humans on the grounds of their skewed or squared outline configurations, respectively. However, the overlapping area between both species is larger in this case. Irrespectively of whether enamel cracks are corrected or not, the Axlor M^1 plots again in the area of overlapping of both species. Outline shape data also classify the Axlor M^1 as a modern human with a very high probability of more than 99% (with and without enamel crack corrections). Form analyses (including size information) also make Axlor M^1 plot comfortably within the range of variation of modern humans.

Ax.13F.265.2 (AX.13E/13F.265-270.2 according to museum records) This tooth is well preserved upper left M^3. The crown is complete, but the lingual root is broken, and it is possible to observe longitudinal cracks on both sides of the preserved root fragment. In addition, it shows moderate wear on the buccal cusp tips but there is no exposed dentine on them (stage 2; Molnar, 1971).

There is a well-developed metacone but the hypocone is absent (Table 5). Nevertheless, there is a small fifth cusp, that is positioned distally to a lingual tubercle. On the EDJ it can be observed that there is no crista obliqua, and that the post-paracone tubercle is intermediate (Table 5). Dentine horn tips of the major cusps are not centrally compressed. The preserved part of the root corresponds to the two buccal roots, with both apical tips completely closed. These two roots are fused, but the root canals run independently along most of the root, except in the most apical tip where they meet again.

[INSERT TABLE 5 HERE]

Shape analyses show that the separation between Neandertal and modern human M^3s is far from clear (Figure 6; Gómez-Robles et al., 2012). Both species overlap completely along PC1, and they show certain morphological trends only along PC2, with Neandertals tending to show positive values associated with a more expanded hypocone, and modern humans tending to show negative values associated with a strongly reduced hypocone that may be absent altogether. As with the other adult posterior teeth, the M^3 from Axlor plots on the area of the morphospace where Neandertals and modern humans overlap. Shape data classify this M^3 as a modern human with a probability of 78.4%, but it should be noted that the percentage of correct classification for Neandertals is very low. The inclusion of size information makes this molar plot far outside the range of variation of Neandertals on the grounds of its small size.

In summary, based on both morphological and size characteristics, this individual shows stronger affinities with modern humans than with Neandertals.

3.3-Additional dental remains

AX.5B.299.16 This is a well-preserved lower right first incisor, although it shows heavy wear on the incisal edge, having lost between the 20-50% of the crown (roughly equivalent to Grade 4; Molnar, 1971; Figure 7). The degree of shoveling, labial convexity and the interproximal facets cannot be assessed due to the heavy incisal wear. The bucco-lingual diameter (7.7 mm) is larger than the one observed in modern humans and it fits well within the Neandertal range of variation. In contrast, the mesio-distal diameter is slightly smaller than the Neandertal minimum and falls within the modern human distribution (Table 2). Nonetheless, this mesio-distal measure is most probably affected by the wear of the crown. The cingular region is bulky, although there is no tuberculum dentale. The heavy wear also affects the observation of the degree of shoveling at the EDJ level, where no tuberculum dentale is observed. The root length of this incisor is 20.86 mm, equal to the maximum value reported in Neandertals (13.8-20.86 mm), and longer than the currently known values for Upper Palaeolithic (11.84-14.20 mm) and recent modern humans (13.18-19.22 mm) (comparative samples from Le Cabec et al., 2013). In addition, the root volume is higher than any reported value for Neandertals or anatomically modern humans (458.33 mm^3). On the other hand, the volume of the crown pulp (CrPV) and the radicular canal (RpV) are in the low end of the variability of Neandertals, 6.61 mm^3 and 2.65 mm^3, respectively. The ratio between the volume of these two values is 0.4, which is situated in the highest half of the Neandertal variability, indicating a proportionally bigger crown pulp segment compared to the root (comparative samples from Le Cabec et al., 2013). In sum, the features observed on this tooth (in particular, its crown and root length size) align it with Neandertals.

[INSERT FIGURE 7 HERE]

AX.5B.299.31.64.17 This is an upper left first deciduous incisor with a well-preserved crown, but the root is not complete (Figure 7). The smooth and twisted aspect of the fracture line of the root has been interpreted in other individuals as the result of root resorption, corresponding to a 6-8-years-old individual based on modern standards (AlQahtani, Hector, & Liversidge, 2010). Despite the heavy wear (Grade 5, Molnar, 1971), a marked shovel shape is observable on the enamel surface (>3 ASUDAS). The mesio-distal diameter of this incisor falls within the metric variation of both Neandertals and modern humans, but the bucco-lingual diameter is larger than the maximum value for the latter group (Table 2). There is no tuberculum dentale, and it is not possible to evaluate the labial convexity on the enamel. The EDJ shows a strong and asymmetric labial convexity, more marked on the mesial side than on the distal. Moreover, there is no tuberculum dentale observed at the EDJ level, and it shows a well-developed shovel shape (>3 ASUDAS). In sum, the features observed on this tooth (in particular, its strong and asymmetric labial convexity, its well-developed shovel shape) and its size align it with Neandertals.

AX.9E.283.103 This tooth is an upper left second deciduous molar that preserves a nearly complete crown. The tooth is heavily worn exhibiting dentine in all four cusps, and the mesial inter-proximal side of the enamel is missing. This tooth does not preserve the root, likely resorpted and/or subsequently broken, and would have belonged to a 10-11-years-old individual based on modern standards (AlQahtani et al., 2010). The size of the crown of this specimen does not provide taxonomic information due to the large overlap between Neandertals and modern humans (Table 2). Both the metacone and the hypocone are well developed (grade 4 ASUDAS). Despite the heavy wear, it is possible to observe a big Carabelli's trait (Grade > 2 ASUDAS), but it is not possible to assess the presence of any other accessory tubercles. The EDJ presents a big Carabelli's trait that is affected by the fracture of the mesial interproximal side of the tooth, which does not allow locating the dentine horn. Moreover, the crista obliqua is continuous, and of type II, with a centered placed

protocone, which is a typical Neandertal trait (Becam et al., 2015; Becam & Chevalier, 2019). A quantitative analysis of this molar has not been carried out, but qualitative observation shows that the skewed morphology typical of Neandertal dm^2s is not present (Bailey et al., 2014). A generally squared outline morphology is present in this specimen instead. This squared morphology may result from the presence of a well-developed Carabelli's trait, which is reported to give Neandertal dm^2s a less skewed appearance (Bailey et al., 2014). In sum, most features observed on this tooth align it with Neandertals.

Discussion

Taxonomic assessment of the Axlor fossil remains

The human remains from Axlor can be divided into two different groups. The first group includes a series of published dental remains, traditionally regarded as belonging to a single Neandertal individual (Basabe, 1973), which our results better classify as belonging to a modern human. Indeed, a detailed evaluation of the field notes of J.M. Barandiarán and our own assessment of the stratigraphy at the place where these remains were found cast doubts regarding their belonging to the Middle Paleolithic layers (Supplementary Information Text S1). The second group of human remains includes three dental remains and a cranial fragment, described here for the first time, which show clear Neandertal affinities and whose attribution to Mousterian layers seems secure based on our assessment of the J.M. Barandiarán field notes.

The first group includes three teeth, P^4, M^1 and M^3 (plus two additional lost specimens), likely belonging to the same individual as already stated by Basabe (1973). The (moderate) wear stage and the fact that the apical tip of the M^3 root is closed indicates that they belonged to a young adult. Several features, mainly related to the M^1 morphology, question the previous taxonomic

assignment of these teeth. First, the hypocone of the M^1 is not bulky and projected disto-lingually (Figures 5-6; Supplementary Information Figures S14-S15), the tips of the dentine horns, as far as it can be inferred given the heavy wear of the molar, are not centrally placed, and the molar is not taurodont. In summary, this molar lacks all the traits that are typically associated with Neandertal M^1s. Second, the P^4 shows a single root channel (an infrequent trait in Neandertals; Pan & Zanolli, 2019), a reduced lingual cusp and a shortened interfoveal distance (typically observed in modern humans). However, other traits in this individual seem to be more frequent in Neandertals. First, the bifurcated buccal and lingual essential crests on the P^4 EDJ and the continuous transverse crest are typically Neandertal features (Becam et al., 2019), as it is a generally asymmetric P^4 crown (Gómez-Robles et al., 2011). Second, the presence of crista obliqua is a Neandertal M^3 common feature (Martin et al., 2017), but the Axlor specimen does not present it in any typology. Moreover, in this M^3 only the metacone dentine horn tip is slightly centrally placed, while the rest of the cusps show the typical morphology of *Homo sapiens*. However, it should be noted that variation of UPMH in many of these traits is not completely understood (e.g., for the P^4, there is only information from one UPMH; Becam et al., 2019). Moreover, the discovery of UPMH with evidence of recent Neandertal admixture (Fu et al., 2015) and the mounting evidence that Neandertal-modern human hybridization may have been common could partially explain the differences found between the dental morphology of the UPMH and Holocene populations.

In addition, a qualitative assessment of the teeth that are now lost from the collection (C* and M^2), based on the information and figures provided by Basabe (1973), indicates that they likely belonged to the same individual due to the overall morphology and wear degree compatibility. Moreover, the M^3 presents a small interproximal facet, compatible with the M^2 with reduced hypocone presented by Basabe (1973). Regarding the morphology of these two lost teeth, it is possible to observe on the original publication that the upper canine has some archaic features: a bulky tuberculum linguale (ASUDAS grade >3) and well developed mesial ridge (grade 2), more

common in Neandertals (100% and 42.1%, respectively) and UPMHs (40% and 11.1%, respectively) than in recent *Homo sapiens* (8% and 5.3%, respectively) (Martinón-Torres et al., 2012). On the other hand, the M^2 presents a large metacone (ASUDAS grade 3-4), a reduced hypocone (ASUDAS grade 0-2), and absence of Carabelli's tubercle (ASUDAS grades 0-1). Reduced hypocones are more common in UPMHs (50%) than in Neandertals (24.9%) (Martinón-Torres et al., 2012).

Based on this morphological information, the absence of Holocene recent prehistory remains from the Axlor sequence, the presence of an early Upper Paleolithic occupation in the site (González-Urquijo et al., 2014), and the unclear previous ascription to the Mousterian level III due to their finding in loose sediment close to the rock-shelter wall (see Supplementary information), we hypothesize that these human remains could belong to an UPMH, which should be tested in the near future using direct C14 datings. Currently, except for a few skeletons (Lagar Velho, Mirón; Duarte et al., 1999; Carretero et al., 2015) most of the Upper Paleolithic remains from the Iberian Peninsula consist of isolated teeth or cranial remains (Pérez Iglesias, 2007, and references therein).

We consider that the stratigraphic ascription of these teeth, rather than their morphology *per se*, have contributed to incorrectly classify the published teeth from Axlor as belonging to Neandertals. While Basabe (1973) considers that their general morphology resembles that of other individuals found in Mousterian contexts, he still underlines their "evolved" status with the presence of "intermediary characters" (Basabe, 1973:200), especially refering to the low degree of taurodontism in the M^1 and the M^2. The same author did classify the M^1 from Lezetxiki, which shows the typical Neandertal occlusal morphology and a clear taurodontism (Basabe, 1970), as belonging to a Neandertal individual.

The second study that classified the Axlor teeth as Neandertals compared them with Sima de los Huesos, Neandertals and modern humans both morphologically (using the data by Martinón-Torres et al., 2012) and metrically (using the data by Rodríguez-Cuenca (2003) and García-Bour, Pérez-Pérez, & Chimenos (1997). However, most traits included in that study (Rostro-Carmona,

2013) are not taxonomically distinctive and, for those which are, the Axlor teeth show modern human affinities. In terms of size, and using the data provided by Rostro-Carmona (2013), only the canine would show a size closer to the Neandertal mean, the P^4 and M^1 would show intermediate affinities while the size of the M^2 and M^3 would be more similar to modern humans. Our study shows that, after including UPMHs in the comparative samples, and despite the overlap between modern humans and Neandertals, the general size of the Axlor teeth is either non-determinant or more similar to modern humans. Finally, Rostro-Carmona (2013) used the presence of taurodontism in the Axlor teeth to classify them as belonging to Neandertals, but our assessment indicates that the Axlor teeth show a very limited degree of taurodontism, particularly when compared with classic Neandertal molars.

The second group would encompass the cranial fragment and three additional tooth remains that have clear Neandertal affinities and their stratigraphic position is secure within the Mousterian levels. The bone thickness distribution pattern and endocranial anatomy of the cranial remain are consistent with Neandertal anatomy. Additionally, both incisors and the dm^2 present characteristics that allow us to ascribe them to Neandertals. Although heavily worn, the I_1 shows Neandertal affinities in its root configuration and proportions. Nevertheless, the CrPV and RpV values are lower than the Neandertal values reported to date (Le Cabec et al., 2013; Becam & Chevalier, 2019). This might be related to an advanced age for the individual, as aging related deposition of secondary dentine causes the reduction of the pulp channel (Aboshi, Takahashi, & Komuro, 2010; Solheim, 1992). This would be consistent with the heavy wear present in this tooth. Second, both the OES and EDJ of the deciduous upper incisor from Axlor present a set of characteristics observed in other Neandertal specimens such as Portel-Ouest, La Ferrassie 8 (strong mesial and distal marginal ridges, pronounced and asymmetric labial convexity) (Becam & Chevalier, 2019). Third, although the dm^2 does not show the typical Neanderthal skewed configuration, it does show a notable development of the hypocone in relation to the metacone, the presence of the crista obliqua, and a large Carabelli's tubercle at the OES and EDJ. These are common features to other

Neandertal dm^2s, such as Arrillor, La Ferrassie 8 or Portel-Ouest (Becam & Chevalier, 2019; Bermúdez de Castro & Saenz de Buruaga, 1999). These new remains confirm the presence of Neandertal fossil remains in Axlor, thus increasing the Neandertal hypodigm recovered in the Eastern Cantabrian Region.

Origin of the accumulation of the human fossil remains

Taphonomic and forensic analyses on hominin fossils are important to determine the origin of bone deposition and reconstruct the processes occurred during the fossil-diagenetic processes even for isolated fossils (Sanz et al., 2018). In some cases, it is even possible to determine causes of death (Sala et al., 2015) or drawing inferences about the mortuary practices of hominin groups, such as cannibalism (Rougier et al., 2016; Sala & Conard, 2016; Saladié et al., 2012; Saladié & Rodríguez-Hidalgo, 2017) or funerary activities (Gómez-Olivencia et al., 2018b).

In the case of the two deciduous teeth, they were lost by two different Neandertal individuals during the formation of levels V (left di^1) and IV (right dm^2). The presence of isolated deciduous teeth is not rare in Middle Paleolithic layers, and the closest example is found less than 25 km south from Axlor, in Arrillor (Figure 1; Bermúdez de Castro & Saénz de Buruaga, 1999; Iriarte-Chiapusso, Wood, & Sáenz de Buruaga, 2019), with other example from Le Portel Ouest (Becam & Chevalier, 2019). The cranial fragment from Axlor displays evidence of postmortem and perimortem fractures, but the absence of traces that could indicate the causes of such fractures makes it difficult to interpret its origin. Although we cannot rule out intentional causes for the perimortem fractures, the lack of clear anthropic cut marks or signs of anthropic manipulation does not allow us to go further in our interpretation. The absence of weathering could be interpreted as a non-aerial (or short-term) exposure of the fossils in the biostratinomic phase. On the other hand,

trampling has been documented on the cranial fragment suggesting certain displacement of the fossils which could be one of the explanations of the scarcity of human remains at the site. Additionally, the Barandiarán collection shows some significant bias in comparison with the richness in fossil remains that we have observed at the site during recent excavations (Gómez-Olivencia et al., 2018a), in which smaller shaft fragments are absent. This bias could be a secondary reason of this scarcity. In this context, the recovery of additional human fossils in the Axlor site would help elucidate the nature of these isolated remains found in a human occupation context.

Conclusions

Axlor (Dima, Biscay) is one of the most important Middle Paleolithic sites in the Cantabrian region (northern Iberian Peninsula). The excavations performed by J.M. Barandiarán at the Axlor site 50 years ago yielded a cranial vault fragment and eight teeth, five of which likely belonged to the same individual, although two are currently lost. Three teeth (a left dm^2, a left di^1, and a right I_1) and the cranial fragment show morphological features consistent with their classification as Neandertals, and were found in undisturbed Mousterian context. However, the remaining three teeth (plus two that have been lost since the initial finding), traditionally classified as Neandertals (Basabe, 1973; Rostro Carmona, 2013), show morphological features and a general size more compatible with their classification as modern humans. Moreover, the review of the original notes by J.M. Barandiarán and our own observations during the recent excavations at the site suggest that the archaeological context of these remains should be carefully reconsidered. We hypothesize that these teeth may constitute one of the scarce examples of Upper Paleolithic remains in the Iberian Peninsula, a hypothesis that would require a direct C14 dating to be tested, which currently is not possible due to access limitations.

ACKNOWLEDGMENTS

We would like to thank I. García Camino (Arkeologi Museoa) for permission to study these fossils. We thank L. García Boullosa for the cleaning of some of these fossils, and to the rest of the Arkeologi Museoa staff. The Gobierno Vasco-Eusko Jaurlaritza granted the permission to micro-CT these specimens. Thanks to the Jose Miguel de Barandiaran Fundazioa and Zuriñe Velez de Mendizabal for the access to J.M. de Barandiarán's field notes. Thanks to B. Notario (CENIEH) for help during the micro-CT scanning process. This research has also received support from the Spanish Ministerio de Ciencia, Innovación y Universidades (proyecto PGC2018-093925-B-C33), Research Group IT1418-19 from the Eusko Jaurlaritza-Gobierno Vasco. NS was supported by a Juan de la Cierva Incorporación program (IJCI-2017-32804). Thanks also to our colleagues from BBP, UCM-ISCIII, EHU-UPV, as well as to A. Rodríguez-Hidalgo and N. Weaver for stimulating discussions.

ORCID

Asier Gómez-Olivencia https://orcid.org/0000-0001-7831-3902

Diego López-Onaindia https://orcid.org/0000-0002-5266-6416

Nohemi Sala https://orcid.org/0000-0002-0896-1493

Antoine Balzeau https://orcid.org/0000-0002-4226-611X

Ana Pantoja

Ignacio Arganda-Carreras https://orcid.org/0000-0003-0229-5722

Mikel Arlegi http://orcid.org/0000-0001-5665-9275

Joseba Rios-Garaizar https://orcid.org/0000-0001-8474-2156

Aida Gómez-Robles https://orcid.org/0000-0002-8719-2660

REFERENCES

Aboshi, H., Takahashi, T., & Komuro, T. (2010). Age estimation using microfocus X-ray computed tomography of lower premolars. *Forensic Science International*, *200*, 35-40.

Albisu Andrade, C., Etxeberria Gabilondo, F., & Herrasti Erlogorri, L. (2014). Estudio de los restos dentales humanos procedentes de la cueva de Santa Catalina. In E. Berganza Gochi, & J. L. Arribas Pastor (Eds.). La Cueva de Santa Catalina (Lekeitio): La intervención arqueológica Restos vegetales, animales y humanos, (pp. 361-365). Bilbao: Bizkaiko Foru Aldundia.

Altuna, J. (1989). La subsistance d'origine animal pendant le Moustérien dans la région Cantabrique (Espagne). In M. Pathou, & L. G. Freeman (Eds.). L'Homme de Neandertal La Subsistance Actes du Colloque International de Liège, vol 6, (pp. 41-43). Liège: ERAUL.

AlQahtani, S.J., Hector, M.P., & Liversidge, H.M. (2010). The London atlas of human tooth development and eruption. *American Journal of Physical Anthropology*, *142*, 481-490.

Arambourou, R., & Genet-Varcin, R. (1965). Nouvelle sépulture du Magdalénien final dans la grotte Duruthy à Sorde-l'Abbaye (Landes): Masson.

Arganda-Carreras, I., Kaynig, V., Rueden, C., Schindelin, J., Eliceiri, K. W., Cardona, A., & Sebastian Seung, H. (2017). Trainable Weka Segmentation: a machine learning tool for microscopy pixel classification. *Bioinformatics*, *33*, 2424-2426.

Bayle, P., Le Luyer, M., & Robson Brown, K. A. (2017). The Palomas Dental Remains: Thickness and Tissue Proportions. In E. Trinkaus, & M. J. Walker (Eds.). Neandertals from the Sima de las Palomas del Cabezo Gordo, Southeastern Spain, (pp. 115-137). College Station, Texas: Texas A&M University Press.

Bailey, S. E. (2002). A closer look at Neanderthal postcanine dental morphology: The mandibular dentition. *The Anatomical Record*, *269*, 148-156.

Bailey, S. E. (2004). A morphometric analysis of maxillary molar crowns of Middle-Late Pleistocene hominins. *Journal of Human Evolution*, *47*, 183-198.

Bailey, S. E., Benazzi, S., Souday, C., Astorino, C., Paul, K., & Hublin, J.-J. (2014). Taxonomic differences in deciduous upper second molar crown outlines of *Homo sapiens*, *Homo neanderthalensis* and *Homo erectus*. *Journal of Human Evolution*, *72*, 1-9.

Balzeau, A. (2013). Thickened cranial vault and parasagittal keeling: Correlated traits and autapomorphies of *Homo erectus*? *Journal of Human Evolution*, *64*, 631-644.

Balzeau, A., Buck, L. T., Albessard, L., Becam, G., Grimaud-Hervé, D., Rae, T. C., & Stringer, C. B. (2017). The Internal Cranial Anatomy of the Middle Pleistocene Broken Hill 1 Cranium. *PaleoAnthropology*, *2017*, 107-138.

Balzeau, A., Grimaud-Hervé, D., & Gilissen, E. (2011). Where are inion and endinion? Variations of the exo- and endocranial morphology of the occipital bone during hominin evolution. *Journal of Human Evolution*, *61*, 488-502.

Barandiarán, I., & Cava, A. (2008). Identificaciones del Gravetiense en las estribaciones occidentales del Pirineo: modelos de ocupación y uso. *Trabajos de Prehistoria*, *65*, 13-28.

Barandiarán, J. M. (1980). Excavaciones en Axlor. 1967-1974. In J. M. Barandiarán (Ed.). Obras Completas de José Miguel de Barandiarán Tomo XVII, (pp. 127-384). Bilbao: La Gran Enciclopedia Vasca.

Basabe, J. M. (1970). Dientes humanos del paleolítico de Lezetxiki (Mondragón). *Munibe*, *XXII*, 113-124.

Basabe, J. M. (1973). Dientes humanos del Musteriense de Axlor (Dima. Vizcaya). *Trabajos de Antropología*, *16*, 187-207.

Basabe, J. M. (1982). Restos fósiles humanos de la región Vasco-Cantábrica. *Cuadernos de Sección Antropología-Etnografía*, *1*, 67-84.

Becam, G., Chevalier, T., Gregoire, S., Braga, J., Balzeau, A., De Lumley, M.A., Vezian, R. 2015. The characterization of the outer enamel surface and the enamel dentine junction of deciduous and permanent Neandertal teeth from Le Portel-Ouest cave (Ariège, France). *1840ème Journée de la Societé d'Anthropologie de Paris*.

Becam, G., & Chevalier, T. (2019). Neandertal features of the deciduous and permanent teeth from Portel-Ouest Cave (Ariège, France). *American Journal of Physical Anthropology*, *168*, 45-69.

Becam, G., Verna, C., Gómez-Robles, A., Gómez-Olivencia, A., Albessard, L., Arnaud, J., . . . Balzeau, A. (2019). Isolated teeth from La Ferrassie: Reassessment of the old collections, new remains, and their implications. *American Journal of Physical Anthropology*, *169*, 132-142.

Behrensmeyer, A. K. (1978). Taphonomic and ecologic information from bone weathering. *Paleobiology*, *4*, 150-162.

Bermúdez de Castro, J. M., & Sáenz de Buruaga, A. (1999). Étude Préliminaire du site Pléistocène Supérieur à hominidé d'Arrillor (Pays Basque, Espagne). *L'Anthropologie*, *103*, 633-639.

Carlsen, O. (1987). Dental Morphology. Copenhagen: Munksgaard.

Carretero, J. M., Quam, R. M., Gómez-Olivencia, A., Castilla, M., Rodríguez, L., & García-González, R. (2015). The Magdalenian human remains from El Mirón Cave, Cantabria (Spain). *Journal of Archaeological Science*, *60*, 10-27.

Castaños, P. M. (2005). Revisión actualizada de las faunas de macromamíferos del Würm antiguo en la Región Cantábrica. In J. A. Lasheras, & R. Montes (Eds.). Neandertales cantábricos, estado de la cuestión, (pp. 201-207). Santander: Museo de Altamira.

de la Rúa, C., & Hervella, M. (2011). Estudio antropológico de los dientes humanos de la cueva de Aitzbitarte III (Rentería. Gipuzkoa) (Paleolítico superior). In J. Altuna, K. Mariezkurrena, & J. Rios (Eds.). Ocupaciones humanas en Aitzbitarte III (País Vasco) 33600-18400 BP (Zona de entrada a la cueva), (pp. 385-393). Vitoria-Gasteiz: Eusko Jaurlaritza-Gobierno Vasco.

Domínguez-Rodrigo, M., de Juana, S., Galán, A. B., & Rodríguez, M. (2009). A new protocol to differentiate trampling marks from butchery cut marks. *Journal of Archaeological Science*, *36*, 2643-2654.

Duarte, C., Maurício, J., Souto, P., Pettitt, P. B., Trinkaus, E., Van Plicht, H. D., & Zilhão, J. (1999). The early Upper Paleolithic human skeleton from the Abrigo do Lagar Velho (Portugal) and modern human emergence in Iberia. *Proceedings of the National Academy of Sciences of the United States of America*, *96*, 7604-7609.

Fu, Q., Hajdinjak, M., Moldovan, O. T., Constantin, S., Mallick, S., Skoglund, P., . . . Pääbo, S. (2015). An early modern human from Romania with a recent Neanderthal ancestor. *Nature*, *524*, 216-219.

García-Bour, J., Pérez-Pérez, A., & Chimenos, E. (1997). Evolución de la dentición en la transición mesolítico-neolítico de la península ibérica; un modelo de sustitución poblacional. *Anales de Odontoestomatología*, *3*, 116-121.

Garralda, M. D. (2005). Los Neandertales en la Península Ibérica. *Munibe (Antropologia Arkeologia)*, *57*, 289-314.

Garralda, M.-D., Maíllo-Fernández, J.-M., Higham, T., Neira, A., & Bernaldo de Quirós, F. (in press). The Gravettian child mandible from El Castillo Cave (Puente Viesgo, Cantabria, Spain). *American Journal of Physical Anthropology*. https://doi.org/10.1002/ajpa.23906

Gómez-Olivencia, A., Quam, R., Sala, N., Bardey, M., Ohman, J. C., & Balzeau, A. (2018b). La Ferrassie 1: New perspectives on a "classic" Neandertal. *Journal of Human Evolution*, *117*, 13-32.

Gómez-Olivencia, A., Sala, N., Núñez-Lahuerta, C., Sanchis, A., Arlegi, M., & Rios-Garaizar, J. (2018a). First data of Neandertal bird and carnivore exploitation in the Cantabrian Region (Axlor; Barandiaran excavations; Dima, Biscay, Northern Iberian Peninsula). *Scientific Reports*, *8*, 10551.

Gómez-Robles, A., Bermúdez de Castro, J. M., Martinón-Torres, M., Prado-Simón, L., & Arsuaga, J. L. (2012). A geometric morphometric analysis of hominin upper second and third molars, with particular emphasis on European Pleistocene populations. *Journal of Human Evolution*, *63*, 512-526.

Gómez-Robles, A., Martinón-Torres, M., Bermúdez de Castro, J. M., Margvelashvili, A., Bastir, M., Arsuaga, J. L., . . . Martínez, L. M. (2007). A geometric morphometric analysis of hominin upper first molar shape. *Journal of Human Evolution*, *53*, 272-285.

Gómez-Robles, A., Martinón-Torres, M., Bermúdez de Castro, J. M., Prado-Simón, L., & Arsuaga, J. L. (2011). A geometric morphometric analysis of hominin upper premolars. Shape variation and morphological integration. *Journal of Human Evolution*, *61*, 688-702.

González Echegaray, J., & Freeman, L. G. (1973). Cueva Morín: Excavaciones 1969. Santander: Publicaciones del Patronato de las Cuevas Prehistóricas de la Provincia de Santander.

González Echegaray, J., García Guinea, M. A., Begines Ramírez, A., & Madariaga de la Campa, B. (1963). Cueva de la Chora (Santander). Madrid: Ministerio de Educación Nacional. Dirección General de Bellas Artes. Servicio Nacional de Excavaciones Arqueológicas.

González Echegaray, J., & Ripoll Perelló, E. (1954). Hallazgos en la cueva de La Pasiega (Puente Viesgo, Santander). *Ampurias*, *XV-XVI*, 43-65.

González-Urquijo, J. E., Ibañez, J. J., Lazuén, T., & Mozota, M. (2014). Axlor. In R. Sala (Ed.). Los Cazadores Recolectores Del Pleistoceno Y Del Holoceno En Iberia Y El Estrecho de Gibraltar, (pp. 45-48). Burgos: Universidad de Burgos.

Grimaud-Hervé, D. (1997). L'évolution de l'encéphale chez *Homo erectus* et *Homo sapiens*: exemples de l'Asie et de l'Europe: CNRS ed. Paris.

Guerrero Sala, L. A., & Lorenzo Lizalde, J. L. (1981). Antropología física en Rascaño. In J. González Echegaray, & I. Barandiarán Maestu, (Eds.), *El Paleolítico Superior de la Cueva de Rascaño (Santander)* (pp. 278-). Santander: Ministerio de Cultura. Dirección General de Bellas Artes, Archivos y Bibliotecas.

Henry-Gambier, D., Normand, C., & Pétillon, J.-M. (2013). Datation radiocarbone directe et attribution culturelle des vestiges humains paléolithiques de la grotte d'Isturitz (Pyrénées-Atlantiques). *Bulletin de la Société préhistorique française*, *110*, 645-656.

Iriarte-Chiapusso, M. J., Wood, R., & Sáenz de Buruaga, A. (2019). Arrillor cave (Basque Country, northern Iberian Penisula). Chronological, palaeo-environmental and cultural notes on a long Mousterian sequence. *Quaternary International*, *508*, 107-115.

Jarvis, A., Reuter, H. I., Nelson, A., & Guevara, E. (2008). Hole-filled SRTM for the globe Version 4. *available from the CGIAR-CSI SRTM 90m Database (http://srtm csi cgiar org)*, *15*, 25-54.

Le Cabec, A., Gunz, P., Kupczik, K., Braga, J., & Hublin, J.-J. (2013). Anterior tooth root morphology and size in Neanderthals: Taxonomic and functional implications. *Journal of Human Evolution*, *64*, 169-193.

Legland, D., Arganda-Carreras, I., & Andrey, P. (2016). MorphoLibJ: integrated library and plugins for mathematical morphology with ImageJ. *Bioinformatics*, *32*, 3532-3534.

Marín-Arroyo, A. B., Rios-Garaizar, J., Straus, L. G., Jones, J. R., de la Rasilla, M., González Morales, M. R., . . . Ocio, D. (2018). Chronological reassessment of the Middle to Upper Paleolithic transition and Early Upper Paleolithic cultures in Cantabrian Spain. *Plos one*, *13*, e0194708.

Martin, R. M. G., Hublin, J.-J., Gunz, P., & Skinner, M. M. (2017). The morphology of the enamel–dentine junction in Neanderthal molars: Gross morphology, non-metric traits, and temporal trends. *Journal of Human Evolution*, *103*, 20-44.

Martinón-Torres, M., Bermúdez de Castro, J. M., Gómez-Robles, A., Prado-Simón, L., & Arsuaga, J. L. (2012). Morphological description and comparison of the dental remains from Atapuerca-Sima de los Huesos site (Spain). *Journal of Human Evolution*, *62*, 7-58.

Molnar, S. (1971). Human tooth wear, tooth function and cultural variability. *American Journal of Physical Anthropology*, *34*, 175-190.

Obermaier, H. (1925). El hombre fósil. Madrid: Ediciones Istmo.

Pan, L., & Zanolli, C. (2019). Comparative observations on the premolar root and pulp canal configurations of Middle Pleistocene Homo in China. *American Journal of Physical Anthropology*, *168*, 637-646.

Pérez-Iglesias, J. M. (2007). Restos fósiles humanos en el Paleolítico superior de la península ibérica. *Arqueoweb*, *8*, 1-17.

QGIS Development Team, 2009. QGIS Geographic Information System. Open Source Geospatial Foundation. URL http://qgis.org

Rios-Garaizar, J. (2017). A new chronological and technological synthesis for Late Middle Paleolithic of the Eastern Cantabrian Region. *Quaternary International*, *433*, 50-63.

Rodríguez Cuenca, J. V. (2003). Dientes y diversidad humana: avances de la antropología dental. Bogotá: Editora Guadalupe Ltda.

Rostro Carmona, J. (2013). Estudio comparado de las piezas dentales de *Homo neanderthalensis* del yacimiento Musteriense de Axlor (Dima, Vizcaya). *CKQ Estudios de Cuaternario/Kuaternario Ikasketak/Quaternary Studies*, *3*, 91-100.

Rougier, H., Crevecoeur, I., Beauval, C., Posth, C., Flas, D., Wißing, C., . . . Krause, J. (2016). Neandertal cannibalism and Neandertal bones used as tools in Northern Europe. *Scientific Reports*, *6*, 29005.

Sala, N., & Conard, N. (2016). Taphonomic analysis of the hominin remains from Swabian Jura and their implications for the mortuary practices during the Upper Paleolithic. *Quaternary Science Reviews*, *150*, 278-300.

Sala, N., Pantoja-Pérez, A., Arsuaga, J. L., Pablos, A., & Martínez, I. (2016). The Sima de los Huesos Crania: Analysis of the cranial breakage patterns. *Journal of Archaeological Science*, *72*, 25-43.

Saladié, P., Huguet, R., Rodríguez-Hidalgo, A., Cáceres, I., Esteban-Nadal, M., Arsuaga, J. L., . . . Carbonell, E. (2012). Intergroup cannibalism in the European Early Pleistocene: The range expansion and imbalance of power hypotheses. *Journal of Human Evolution*, *63*, 682-695.

Saladié, P., & Rodríguez-Hidalgo, A. (2017). Archaeological Evidence for Cannibalism in Prehistoric Western Europe: from Homo antecessor to the Bronze Age. *Journal of Archaeological Method and Theory*, *24*, 1034-1071.

Sanguino González, J., & Montes Barquín, r. (2005). Nuevos datos para el conocimiento del Paleolítico Medio en el centro de la Región Cantábrica: la cueva de Covalejos (Piélagos, Cantabria). In R. Montes Barquín, & J. A. Lasheras Corruchaga, (Eds.), *Actas de la Reunión científica: Neandertales cantábricos, estado de la cuestión* (pp. 489-538). Santander: Museo Nacional y Centro de Investigación de Altamira. Ministerio de Cultura.

Sanz M., Sala N., Daura J., Pantoja-Pérez A., Santos E, Zilhão J, and Arsuaga JL. (2018). Taphonomic inferences about Middle Pleistocene hominins: The human cranium of Gruta da Aroeira (Portugal). *American Journal of Physical Anthropology*, *167*, 615-627.

Schindelin, J., Arganda-Carreras, I., Frise, E., Kaynig, V., Longair, M., Pietzsch, T., . . . Cardona, A. (2012). Fiji: an open-source platform for biological-image analysis. *Nature Methods*, 9,676.

Solheim, T. (1992). Amount of secondary dentin as an indicator of age. *European Journal of Oral Sciences*, *100*, 193-199.

Tejero, J. M., Avezuela, B., White, R., Ranlett, S., Quam, R., Tattersall, I., & Bernaldo de Quirós, F. (2010). Un pedazo de la Prehistoria cántabra en Nueva York. Las Colecciones de la Cueva de El Castillo (Puente Viesgo, Cantabria) en el American Museum of Natural History (Nueva York, EEUU). *Munibe (Antropologia-Arkeologia)*, *61*, 5-16.

Turner, C. G., Nichol, C. R., & Scott, G. R. (1991). Scoring procedures for key morphological traits of the permanent dentition: the Arizona State University dental anthropology system. In M. Kelley, & C. Larsen (Eds.). Advances in Dental Anthropology, (pp. 13-31). New York: Wiley-Liss.

Vallois, H., & Delmas, L. (1976). Los frontales de la cueva de El Castillo (España). *Trabajos de Prehistoria*, *33*, 113-120.

Zapata, J., Bayle, P., Lombardi, A. V., Pérez-Pérez, A., & Trinkaus, E. (2017). The Palomas Dental Remains: Preservation, Wear, and Morphology. In E. Trinkaus, & M. J. Walker (Eds.), *Neandertals from the Sima de las Palomas del Cabezo Gordo, Southeastern Spain* (pp. 52-88). College Station, Texas: Texas A&M University Press.

Figure legends

FIGURE 1 Location of Axlor (red star) and other Paleolithic sites with human remains in the Center and East of the Cantabrian Region (northern Iberian Peninsula and southwestern France). 1: La Pasiega (González Echegaray & Ripoll Perelló, 1954); 2: Castillo (N; HS; Garralda, 2005; Garralda, Maíllo-Fernández, Higham, Neira, & Bernaldo de Quirós, in press; Obermaier, 1925; Tejero et al., 2010; Vallois & Delmas, 1976; 3 Covalejos (N, HS; Sanguino González & Montes Barquín, 2005); 4: Pendo (Basabe, 1982); 5: Morín (HS; González Echegaray & Freeman, 1973; Obermaier, 1925); 6: Rascaño (Guerrero Sala & Lorenzo Lizalde, 1981); 7: La Chora (González Echegaray, García Guinea, Begines Ramírez & Madariaga de la Campa, 1963); 8: Mirón (HS; Carretero et al., 2015); 9: Arrillor (N, Bermúdez de Castro & Sáenz de Buruaga, 1999); 10: Axlor (N; HS; this work); 11: Lezetxiki (N; Basabe, 1970); 12: Santa Catalina (HS; Albisu Andrade, Etxeberria Gabilondo, & Herrasti Erlogorri, 2014); 13: Aitzbitarte III (HS; de la Rúa & Hervella, 2011); 14: Alkerdi (Barandiarán & Cava, 2008); 15: Isturitz (HS; Henry-Gambier, Normand, & Pétillon, 2013); 16: Duruthy (HS; Arambourou & Genet-Varcin, 1965). N=Neandertal; HS=*Homo sapiens.* Base map made with QGIS 2.18.17 (QGIS Development Team, 2009) with data by Jarvis, Reuter, Nelson, & Guevara (2008).

FIGURE 2 Excavation plan (a) and stratigraphic column (b) of Axlor cave (modified from Gómez-Olivencia et al., 2018a). (a) In the excavation plan the grid system used by J.M. Barandiarán (black square and white numbers) and the excavation area is shadowed in gray. The grid system used by the recent excavations is marked using black letters and numbers and the excavation area is outlined using a thick black line. The dotted line represents the rock-shelter wall when the site was first excavated, during the excavation this wall went back, revealing a possible cave infilling. The colors correspond to the levels to which these remains were attributed based on the notes by

Barandiarán. (b) Synthetic section of the 1967–1974 excavation stratigraphy, drawn from the description of the layers by J. M. Barandiarán (1980). Different levels are marked with different colors, and the human remains are marked by silhouettes.

FIGURE 3 Ax.11B.415.400 left parietal fragment. The original fossil and the 3D model are shown on different views. On the lower row, the approximate location of this fragment is shown on the La Ferrassie 1 Neandertal cranium (left), a thickness map (from 2 to 12 mm) is shown (middle) with PC that correspond to thicker bone where is located the postcentral sulcus and V to a relative thinning produced by the anterior ramus of the meningeal system; and the anatomical features on the endocranial surface (right): including meningeal veins, A = anterior branch, O = obelic branch, and sulcal imprints C = central sulcus, PC = postcentral sulcus.

FIGURE 4 Ectocranial view of the specimen Ax.11B.415.400 with the location of zones a-d, and detailed images of these zones, where striations are located. In some cases, the grooves show a close "V" shape but do not show microstriations. The general morphology of these grooves (see text) make them compatible with trampling marks.

FIGURE 5 Dental remains previously studied by Basabe (1973) and Rostro-Carmona (2013), and likely belonging to the same individual. The teeth are shown in mesial, buccal, distal, lingual (top) and occlusal (bottom) views, together with the results of the enamel segmentation and the EDJ surface morphology. Pulp chamber volumes (in blue) are shown in mesial (P^4, M^1) and lingual (M^2) views. A virtual reconstruction of the teeth in buccal and occlusal views is also provided. Scale bars = 1 cm.

FIGURE 6 Principal components analysis of shape (left column) and form variation (right column), corresponding to the teeth previously studied by Basabe (1973) and Rostro-Carmona

(2013), and likely belonging to the same individual. The Axlor remains have been compared to Neandertals (NEA), fossil *Homo sapiens* (FSAP) and recent *Homo sapiens* (RSAP). In both form and shape space, the Axlor remains align more closely with modern humans. TPS-grids show anatomical variation corresponding to the positive and negative extreme of each PC when all the other PCs are held equal to 0. For M^1 variation, the two data points correspond to Axlor's variation before (darker red) and after (lighter red) correcting the enamel cracks (Supplementary information Figure S13).

FIGURE 7 New dental remains from the Barandiarán collection of Axlor. AX.5B.299.16 (right permanent first lower incisor, I_1): root canal morphology (blue) in mesial view; mesial, buccal, distal, lingual and occlusal views. AX.5B.299.31.64.17 (upper left first deciduous incisor, dI^1): top, mesial, buccal, distal, lingual and occlusal views. AX.9E.283.103 (left dM^2): top, mesial, buccal, distal, lingual and occlusal views. In the virtual reconstructions, enamel is represented in white and dentine in brown. Scale bars = 1 cm

Table 1

Inventory of the Axlor human remains found during the Barandiarán excavations.

Label	Year	Archaeological context[a]	Revised archaeological context	Museum data base (MDB)/Basabe, 1973 (B)	Present study	Figure
Ax.13F.265.1[a] Ax.13E/13F.265-270.3[b]	1967	Level IV (Mousterian)	Doubtful	Neandertal (MDB) Left P^4 (B)	Modern human Left P^4	Figure 5
Ax.13F.265.3[a] Ax.13E/13F.265-270.3[b]	1967	Level IV (Mousterian)	Doubtful	Neandertal (MDB) Left maxillary fragment with M^1 (B)	Modern human Left maxillary fragment with M^1	Figure 5
Ax.13F.265.3[a]	1967	Level IV (Mousterian)	Doubtful	Left M^2(B)	Specimen lost	-
Ax.13F.265.2[a] Ax.13E/13F.265-270.3	1967	Level IV (Mousterian)	Doubtful	Neandertal (MDB) Left M^3 (B)	Modern human Left M^3	Figure 5
Ax.13E.285.3[a]	1967	Level IV (Mousterian)	Doubtful	Left C˙ (B)	Specimen lost	-
Ax.11B.415.9[a] Ax.11B.415.400 (physical label: Ax.11B.415)b	1969	Level VIII (Mousterian)	Mousterian	Human cranial fragment (MDB) Neandertal (MDB)	Neandertal Left parietal bone	Figure 3
Ax.9E.283.103	1973 or 1974	Level IV (Mousterian)	Mousterian	Fauna (indeterminate taxon) (MDB)	Neandertal Right dm^2	Figure 7
Ax.5B.299.31.64.17	1974	Level V (Mousterian)	Mousterian	Human tooth (MDB)	Neandertal Left di^1	Figure 7
Ax.5B.299.16	1974	Level V (Mousterian)	Mousterian	Human tooth (MDB)	Neandertal Adult right I_1	Figure 7

[a] Based on the information provided by J.M. de Barandiarán field notes. The M^1 and the M^2 were found together.

[b] Based on the information provided by the Arkeologi Museoa (Bilbao, Biscay).

** Virtual (not written) label

Table 2

Comparison of external crown metric data between Axlor teeth and Neandertals, Upper Paleolithic modern humans (UPMH), and recent modern humans (RMH).

Tooth	Variable	Axlor			Neandertals[a]					Upper Palaeolithic modern humans[a]					Recent modern humans[a]				
		This study	Rostro-Carmona, 2013	Basabe, 1973	Mean	SD	Min	Max	*n*	Mean	SD	Min	Max	*n*	Mean	SD	Min	Max	*n*
C	M-D	-	-	8.0	8.74	0.67	7.40	10.00	31	8.06	0.58	6.90	9.50	36	7.58	0.43	6.80	8.5	38
	B-L	-	-	9.2	9.92	0.65	8.40	11.40	34	9.02	0.77	7.50	10.74	38	8.26	0.68	7.20	9.4	38
P^4	M-D	6.6	6.7	6.6	7.49	0.78	6.10	8.80	30	6.84	0.52	5.90	7.90	38	6.45	0.46	5.50	7.5	38
	B-L	9.7	9.8	9.7	10.39	0.70	9.00	11.70	34	9.69	0.69	7.50	11.29	38	9.04	0.49	8.10	9.9	38
M^1	M-D	9.8	10.2	10.0	11.61	1.09	9.30	13.60	28	10.71	0.71	8.40	12.30	41	10.03	0.52	8.40	11.4	42
	B-L	11.1	11.2	11.8	12.34	0.70	11.10	14.20	33	12.12	0.63	10.00	13.98	42	11.27	0.56	10.20	12.5	42
M^2	M-D	-	-	9.3	10.84	1.23	9.10	15.90	34	10.10	0.72	8.90	11.80	41	9.22	0.66	7.80	10.5	41
	B-L	-	-	10.0	12.60	0.94	10.54	14.60	38	12.27	0.90	8.30	14.00	42	11.35	0.84	9.90	13.9	41
M^3	M-D	8.7	8.6	8.6	9.74	0.94	6.80	11.35	30	9.01	1.09	7.00	11.60	39	8.55	0.84	7.30	10.5	30
	B-L	10.2	10.1	10.0	11.96	1.16	7.70	14.25	30	11.40	1.10	6.90	13.30	40	10.88	0.98	9.30	13.2	30
I_1	M-D	4.8	-	-	5.73	0.44	4.92	6.35	24	5.51	0.60	3.70	6.60	22	5.24	0.45	4.60	6.7	31
	B-L	7.7	-	-	7.37	0.51	6.10	8.15	29	6.23	0.45	5.30	7.10	42	6.03	0.44	5.10	6.8	32
di^1	M-D	7.6	-	-	7.03	0.81	5.60	8.00	11	6.85	0.77	6.20	7.70	4					
	B-L	6.0	-	-	5.67	0.48	4.70	6.20	11	5.30	0.29	4.90	5.70	5					
dm^2	M-D	(9.0)	-	-	9.18	0.70	8.00	10.40	15	9.19	0.30	8.97	9.40	2					
	B-L	10.3	-	-	10.14	0.57	9.00	11.10	16	10.32	0.57	9.90	11.10	4					

B-L= Bucco-lingual; M-D = Mesio-distal. Values between parentheses are estimated.

The C*, P^4, M^1, M^2 and M^3 were firstly published by Basabe (2013) and are from the same individual.

[a]For sample information see Supplementary Information Table S5.

Table 3

Comparison of non-metric traits at the occlusal enamel surface (OES), at the enamel-dentine junction (EDJ) and root number between the P^4 and Neandertals, Upper Paleolithic modern humans (UPMH), and recent modern humans (RMH).

Tooth region	Trait	Grade for Axlor	Neandertals		UPMH		RMH	
			n	%	*n*	%	*n*	%
OES	Transverse crest	Absent	2/16	12.4	2/11	18.2	0/113	0.0
	Buccal essential crest (BEF)	2	10/15	66.6	4/11*	36.4	10/106	9.4
	Lingual essential crest (LEF)	NO	11/14	78.6	0/11	0.0	9/108	8.3
	BMaxPAR	1 (Dist)	5/12	41.7	5/9	55.6	18/88	20.5
EDJ	Transverse crest	2 (continuous, but not complete)	9/13	69.2	0/1	0.0	2/14	14.3
	Buccal essential crest	2 (bifurcated)	8/13	61.5	0/1	0.0	4/20	20.0
	Lingual essential crest	2 (bifurcated)	12/13	92.3	0/1	0.0	0/20	0.0
	Distal accesory ridge	1 (present)	5/13	38.4	0/1	0.0	12/20	60.0
	Mesial accesory ridge	0 (absent)	8/13	61.5	1/1	100.0	8/20	40.0
	Mesial accesory cusp	0 (absent)	13/13	100.0	1/1	100.0	20/20	100.0
	Distal accesory cusp	0 (absent)	10/13	76.9	1/1	100.0	20/20	100.0
Root	Root canal type	$1R_1$	1/10	10.0	-	-	4/13	30.8

OES trait frequencies from Martinón-Torres et al. (2012); EDJ data from Becam et al. (2019); Root channel data from Bayle, Le Luyer, & Robson Brown (2017; Las Palomas 53 and 68 left P^4s), Zapata, Bayle, Lombardi, Pérez-Pérez, & Trinkaus (2017), and Pan & Zanolli (2019).

Table 4

Comparison of non-metric traits at the occlusal enamel surface (OES) and enamel-dentine junction (EDJ) between the Axlor M^1, Neandertals, Upper Paleolithic modern humans (UPMH) and recent modern humans (RMH).

Tooth region	Trait	Grade for Axlor	Neandertals		UPMH		RMH	
			n	%	*n*	%	*n*	%
OES	Metacone	4	13/23	56.5	11/19	57.9	73/127	57.5
	Hypocone	4	10/23	43.5	10/19	52.6	58/127	45.7
	Cusp 5	0	1/22	4.5	1/18	5.6	44/125	35.2
	Parastyle	0	14/20	70.0	15/15	100.0	121/123	98.4
EDJ	Crista Obliqua	Type II	2/19	10.0	-	-	1/12	8.3
	Post Paracone	Intermediate	10/19	52.6	-	-	0/12	0.0

OES trait frequencies from Martinón-Torres et al. (2012); EDJ data from Martin et al. (2017; combining data from early and late Neandertals together).

Table 5

Comparison of non-metric traits at the occlusal enamel surface (OES) and enamel-dentine junction (EDJ) between the Axlor M^3, Neandertals, Upper Paleolithic modern humans (UPMH) and recent modern humans (RMH).

Tooth region	Trait	Grade for Axlor	Neandertals		UPMH		RMH	
			n	%	*n*	%	*n*	%
OES	Metacone	>3	9/18	50.0	5/10	50.0	58/93	62.4
	Hypocone	0	3/17	17.6	2/10	20.0	15/93	16.1
	Cusp 5	1	1/17	5.9	1/10	10.0	4/93	4.3
	Carabelli	0	12/15	80.0	5/9	55.6	68/89	76.4
	Parastyle	0	14/16	87.5	9/9	100	81/88	92.0
EDJ	Crista Obliqua	absent	0/12	0.0	-	-	3/7	42.9
	Post Paracone	intermediate	1/12	8.3	-	-	2/7	28.6

OES trait frequencies from Martinón-Torres et al. (2012); EDJ data from Martin et al. (2017; combining data from early and late Neandertals together).

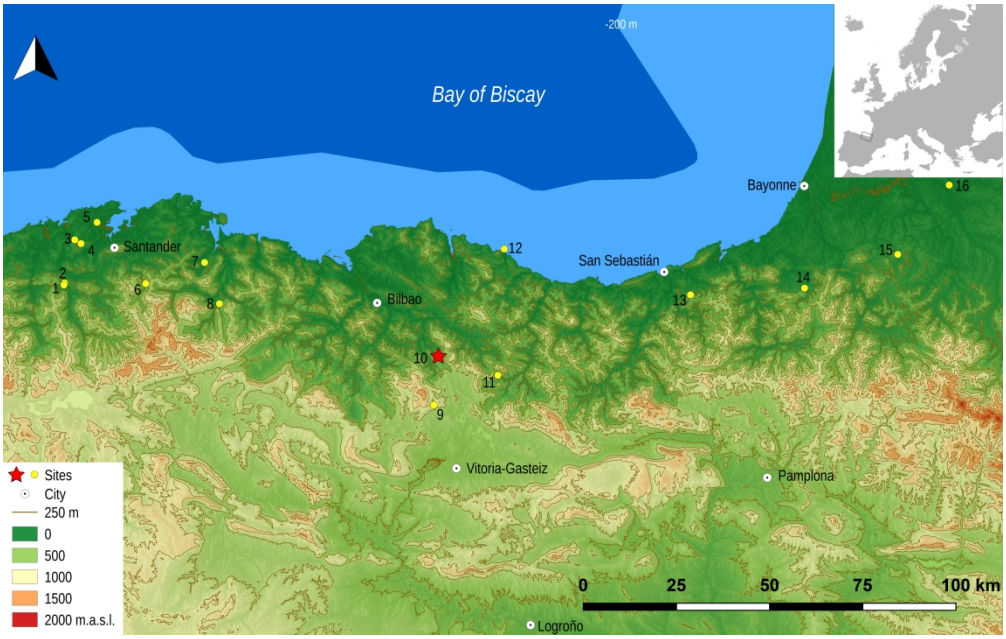

FIGURE 1 Location of Axlor (red star) and other Paleolithic sites with human remains in the Center and East of the Cantabrian Region (northern Iberian Peninsula and southwestern France). 1: La Pasiega (González Echegaray & Ripoll Perelló, 1954); 2: Castillo (N; HS; Garralda, 2005; Garralda, Maíllo-Fernández, Higham, Neira, & Bernaldo de Quirós, in press; Obermaier, 1925; Tejero et al., 2010; Vallois & Delmas, 1976; 3 Covalejos (N, HS; Sanguino González & Montes Barquín, 2005); 4: Pendo (Basabe, 1982); 5: Morín (HS; González Echegaray & Freeman, 1973; Obermaier, 1925); 6: Rascaño (Guerrero Sala & Lorenzo Lizalde, 1981); 7: La Chora (González Echegaray, García Guinea, Begines Ramírez & Madariaga de la Campa, 1963); 8: Mirón (HS; Carretero et al., 2015); 9: Arrillor (N, Bermúdez de Castro & Sáenz de Buruaga, 1999); 10: Axlor (N; HS; this work); 11: Lezetxiki (N; Basabe, 1970); 12: Santa Catalina (HS; Albisu Andrade, Etxeberria Gabilondo, & Herrasti Erlogorri, 2014); 13: Aitzbitarte III (HS; de la Rúa & Hervella, 2011); 14: Alkerdi (Barandiarán & Cava, 2008); 15: Isturitz (HS; Henry-Gambier, Normand, & Pétillon, 2013); 16: Duruthy (HS; Arambourou & Genet-Varcin, 1965). N=Neandertal; HS=Homo sapiens. Base map made with QGIS 2.18.17 (QGIS Development Team, 2009) with data by Jarvis, Reuter, Nelson, & Guevara (2008).

180x113mm (600 x 600 DPI)

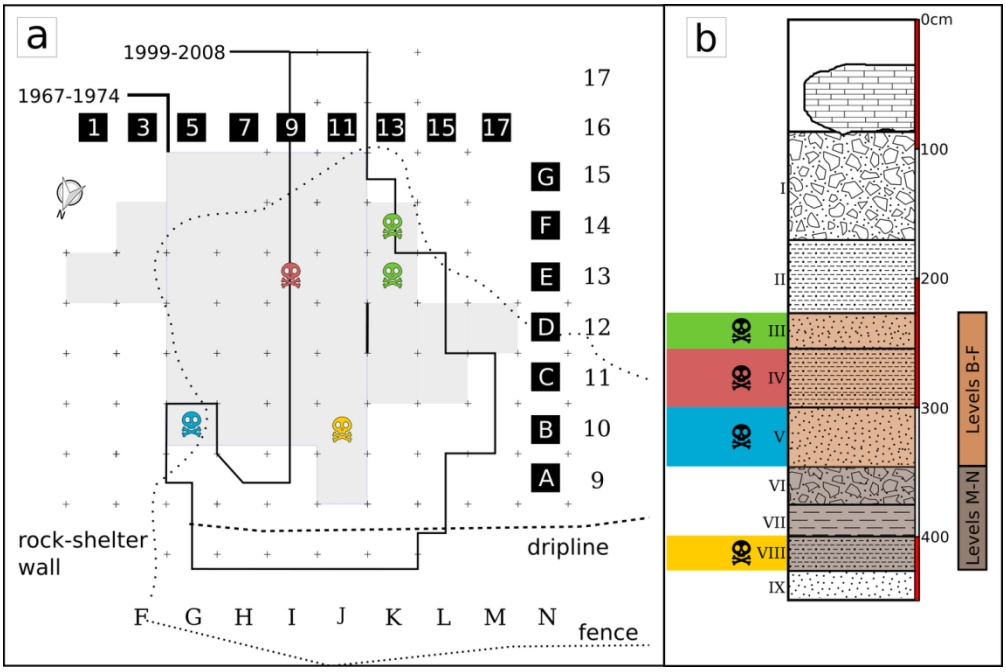

FIGURE 2 Excavation plan (a) and stratigraphic column (b) of Axlor cave (modified from Gómez-Olivencia et al., 2018a). (a) In the excavation plan the grid system used by J.M. Barandiarán (black square and white numbers) and the excavation area is shadowed in gray. The grid system used by the recent excavations is marked using black letters and numbers and the excavation area is outlined using a thick black line. The dotted line represents the rock-shelter wall when the site was first excavated, during the excavation this wall went back, revealing a possible cave infilling. The colors correspond to the levels to which these remains were attributed based on the notes by Barandiarán. (b) Synthetic section of the 1967–1974 excavation stratigraphy, drawn from the description of the layers by J. M. Barandiarán (1980). Different levels are marked with different colors, and the human remains are marked by silhouettes.

132x87mm (300 x 300 DPI)

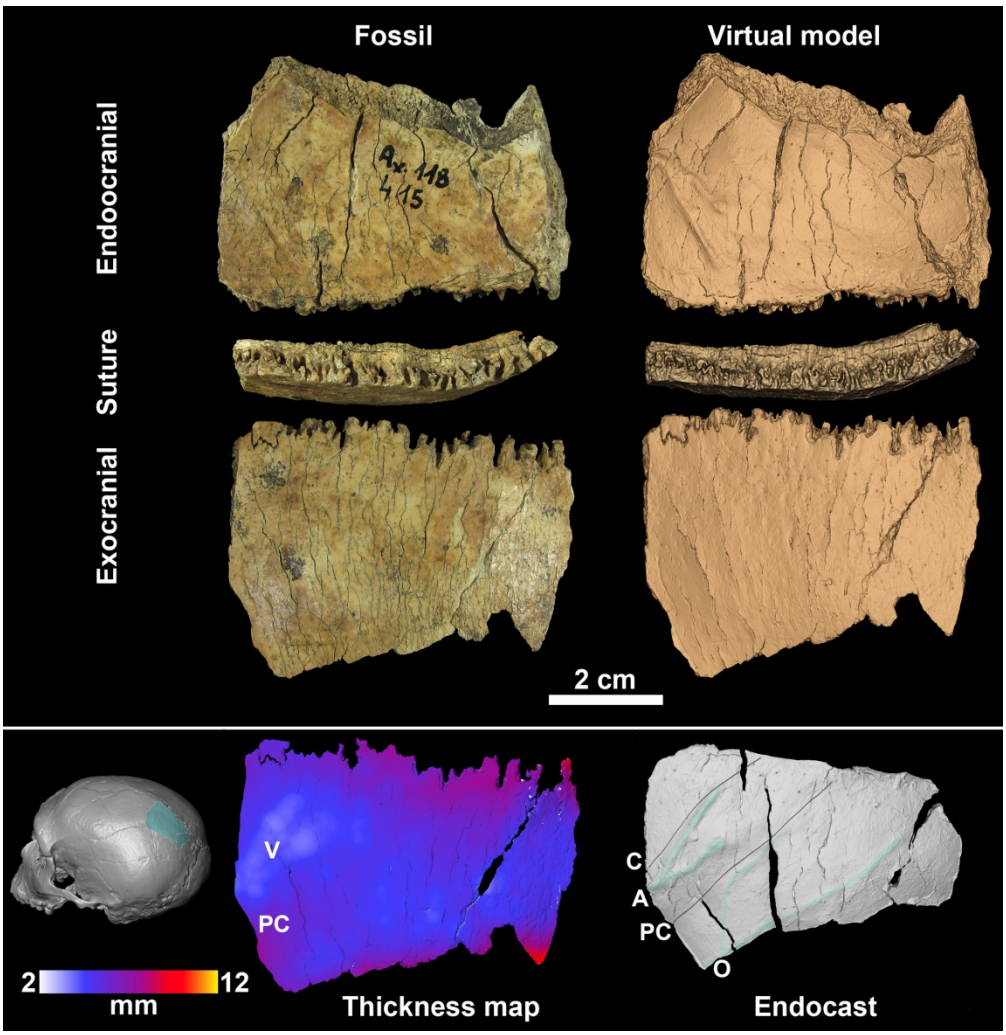

FIGURE 3 Ax.11B.415.400 left parietal fragment. The original fossil and the 3D model are shown on different views. On the lower row, the approximate location of this fragment is shown on the La Ferrassie 1 Neandertal cranium (left), a thickness map (from 2 to 12 mm) is shown (middle) with PC that correspond to thicker bone where is located the postcentral sulcus and V to a relative thinning produced by the anterior ramus of the meningeal system; and the anatomical features on the endocranial surface (right): including meningeal veins, A = anterior branch, O = obelic branch, and sulcal imprints C = central sulcus, PC = postcentral sulcus.

180x184mm (300 x 300 DPI)

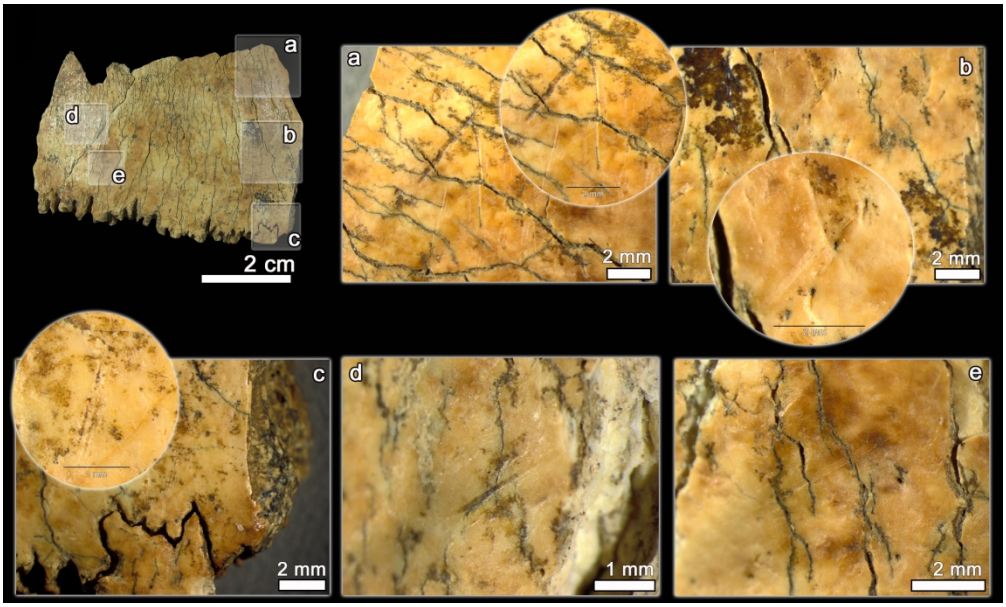

FIGURE 4 Ectocranial view of the specimen Ax.11B.415.400 with the location of zones a-d, and detailed images of these zones, where striations are located. In some cases, the grooves show a close "V" shape but do not show microstriations. The general morphology of these grooves (see text) make them compatible with trampling marks.

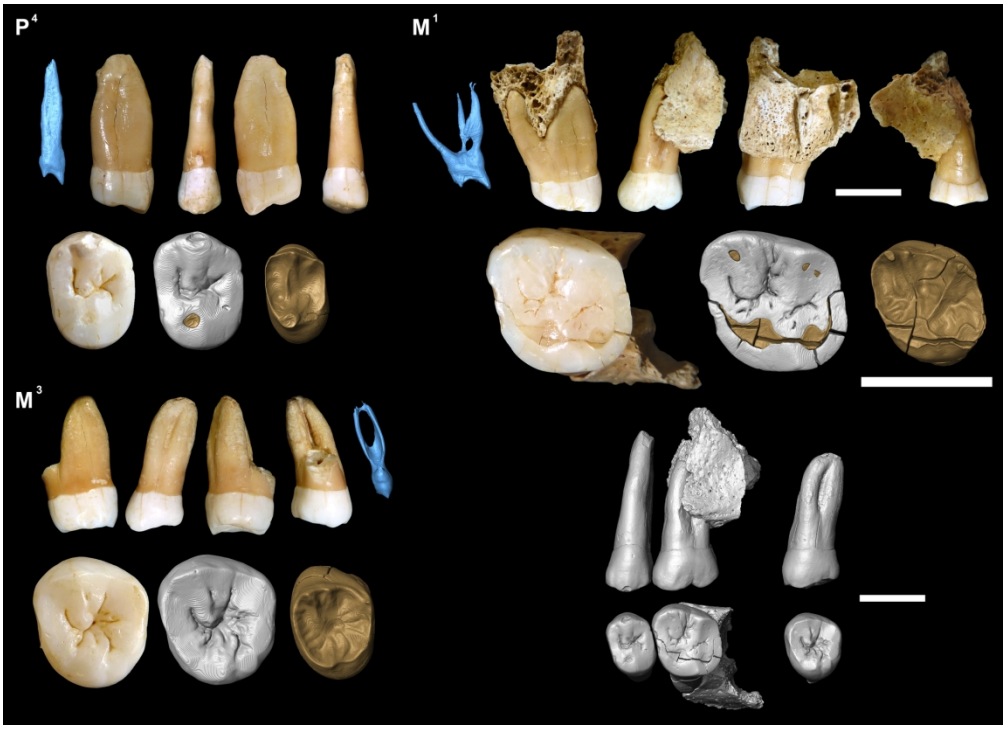

FIGURE 5 Dental remains previously studied by Basabe (1973) and Rostro-Carmona (2013), and likely belonging to the same individual. The teeth are shown in mesial, buccal, distal, lingual (top) and occlusal (bottom) views, together with the results of the enamel segmentation and the EDJ surface morphology. Pulp chamber volumes (in blue) are shown in mesial (P4, M1) and lingual (M2) views. A virtual reconstruction of the teeth in buccal and occlusal views is also provided. Scale bars = 1 cm.

180x129mm (300 x 300 DPI)

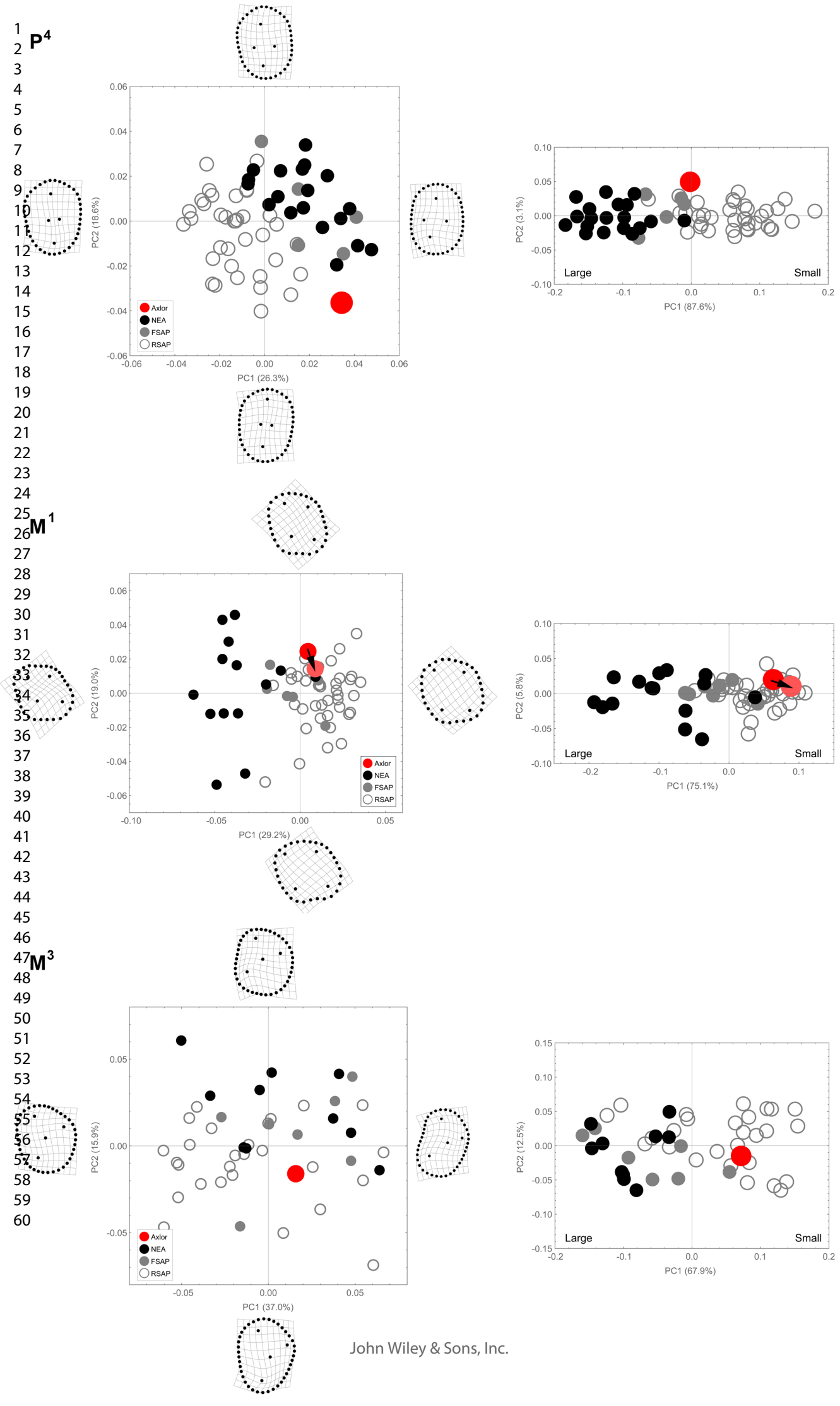
Shape space
Form space
P4
M1
M3
PC1 (26.3%)
PC2 (18.6%)
PC1 (87.6%)
PC2 (3.1%)
PC1 (29.2%)
PC2 (19.0%)
PC1 (75.1%)
PC2 (5.8%)
PC1 (37.0%)
PC2 (15.9%)
PC1 (67.9%)
PC2 (12.5%)
Axlor
NEA
FSAP
RSAP
Large
Small

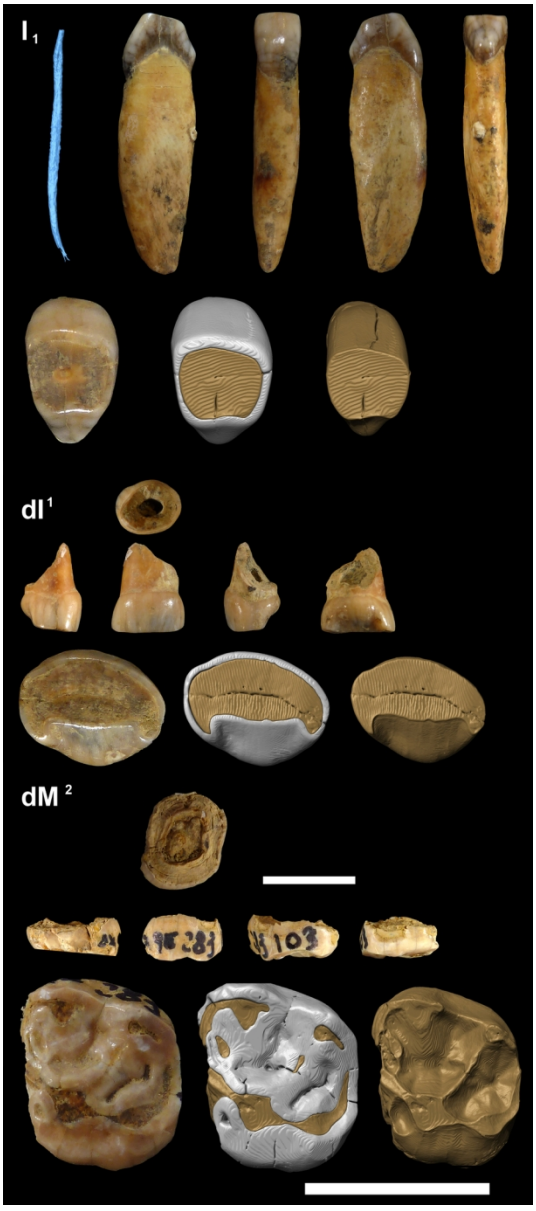

FIGURE 7 New dental remains from the Barandiarán collection of Axlor. AX.5B.299.16 (right permanent first lower incisior, I1): root canal morphology (blue) in mesial view; mesial, buccal, distal, lingual and occlusal views. AX.5B.299.31.64.17 (upper left first deciduous incisor, dI1): top, mesial, buccal, distal, lingual and occlusal views. AX.9E.283.103 (left dM2): top, mesial, buccal, distal, lingual and occlusal views. In the virtual reconstructions, enamel is represented in white and dentine in brown. Scale bars = 1 cm

80x180mm (300 x 300 DPI)